JOURNAL OF GUIDANCE, CONTROL, AND DYNAMICS
Vol. 23, No. 4, July–August 2000

Robust Nonlinear Control of a Hypersonic Aircraft

Qian Wang* and Robert F. Stengel†
Princeton University, Princeton, New Jersey 08544

For the longitudinal motion of a hypersonic aircraft containing 28 inertial and aerodynamic uncertain parameters, robust flight control systems with nonlinear dynamic inversion structure are synthesized. The system robustness is characterized by the probability of instability and probabilities of violations of 38 performance criteria, subject to the variations of the uncertain system parameters. The design cost function is defined as a weighted quadratic sum of these probabilities. The control system is designed using a genetic algorithm to search a design parameter space of the nonlinear-dynamic-inversion structure. During the search iteration, Monte Carlo evaluation is used to estimate the system robustness and cost function. This approach explicitly takes into account the design requirements and makes full use of engineering knowledge in the design process to produce practical and efficient control systems.

Nomenclature

a	= speed of sound, ft/s
C_D	= drag coefficient
C_L	= lift coefficient
$C_M(q)$	= pitching moment coefficient due to pitch rate
$C_M(\alpha)$	= pitching moment coefficient due to angle of attack
$C_M(\delta E)$	= pitching moment coefficient due to elevator deflection
C_T	= thrust coefficient
$\bar{c}$	= reference length, 80 ft
D	= drag, lbf
h	= altitude, ft
I_{yy}	= moment of inertia, 7×10^6 slug-ft^2
J	= cost function
L	= lift, lbf
M	= Mach number
M_{yy}	= pitching moment, lbf-ft
m	= mass, 9375 slugs
q	= pitch rate, rad/s
R_E	= radius of the Earth, 20,903,500 ft
r	= radial distance from Earth's center, ft
S	= reference area, 3603 ft^2
T	= thrust, lbf
V	= velocity, ft/s
α	= angle of attack, rad
α_0	= angle of attack at trim condition, 0.0315 rad
γ	= flight-path angle, rad
δE	= elevator deflection, rad
δT	= throttle setting, %/100
$\boldsymbol{\lambda}$	= vector relative degree
μ	= gravitational constant, 1.39×10^{16} ft^3/s^2
$\boldsymbol{\nu}$	= aerodynamic uncertain parameters vector
ρ	= density of air, slugs/ft^3

I. Introduction

HYPERSONIC flight is very sensitive to changes in flight condition. Furthermore, due to the difficulty in measuring atmospheric properties and estimating aerodynamic characteristics, it is important that the flight control system be robust.

Stochastic robustness analysis[1,2] deals with system parametric uncertainty in a probabilistic way. This approach estimates the likelihood of system instability and violation of performance requirements subject to variations in the probabilistic system parameters. After choosing an appropriate controller structure, stochastic robust control synthesis[3–7] is used to search the design parameter space to minimize a cost that is a function of the probabilities that design criteria will not be satisfied. The framework of stochastic robustness analysis and design can accommodate a wide variety of problems, applicable to systems that are linear or nonlinear, time invariant or time varying. Stochastic robust linear designs of a benchmark problem are presented in Refs. 3–5. Robust nonlinear control synthesis of a simple system with two masses connected by a cubic spring is investigated in Ref. 6.

This paper is part of a continuing effort to develop practical methods for the design of robust flight control systems. In Ref. 7, the linear-quadratic (LQ) stochastic robust control law is designed for a hypersonic aircraft. In this paper, we combine nonlinear dynamic inversion (NDI) with stochastic robustness to produce the control system for this hypersonic aircraft. NDI has drawn considerable attention over the last two decades.[8–10] Control laws that are based on NDI of the aircraft model offer the potential for providing improved levels of performance over linear flight control designs. This is due to the more accurate representation of the forces and moments that arise in response to large state and control perturbations. These control laws also allow specific state variables to be commanded directly, and remain valid over the entire flight envelope without requiring gain scheduling.

In Sec. II, a brief review of the general theory of stochastic robustness and NDI is given. Section III describes the hypersonic aircraft model, and Sec. IV defines the corresponding design metrics. In Sec. V, we design a stochastic robust NDI control for the hypersonic aircraft. Performance analysis of the control system is given in Sec. VI.

II. General Theory of Stochastic Robustness and NDI

A. Stochastic Robustness

Denote a plant structure as $H(\boldsymbol{\nu})$, where $\boldsymbol{\nu}$ is a vector of varying plant parameters selected randomly throughout the parameter space $\boldsymbol{V}$, reflecting the expected distribution $pr(\boldsymbol{\nu})$. Stochastic robustness characterizes a compensator $C(\boldsymbol{d})$ with $\boldsymbol{d}$ as the design parameter, in terms of the probabilities that the closed-loop system will have unacceptable stability and performance when subjected to parametric uncertainties. For each design requirement on stability or performance, define the corresponding binary indicator function $I[\cdot]$ as one if $H(\boldsymbol{\nu})$ and $C(\boldsymbol{d})$ form an unacceptable system and as zero otherwise. Then for each design requirement, the probability of design requirement violation P can be defined as the integral of the corresponding indicator function over the expected system parameter space:

$$P(\boldsymbol{d}) = \int_{\boldsymbol{V}} I[H(\boldsymbol{\nu}), C(\boldsymbol{d})] pr(\boldsymbol{\nu})\, \mathrm{d}\boldsymbol{\nu} \tag{1}$$

Presented as Paper 99-4085 at the AIAA Guidance, Navigation, and Control Conference, Portland, OR, 9–11 August 1999; received 19 August 1999; revision received 20 December 1999; accepted for publication 22 December 1999.

*Graduate Student, Department of Mechanical and Aerospace Engineering. Student Member AIAA.
†Professor, Department of Mechanical and Aerospace Engineering. Fellow AIAA.

The stochastic robustness cost function $J(\boldsymbol{d})$ is formalized by combining the probabilities for different kinds of design requirements with certain tradeoffs:

$$J(\boldsymbol{d}) = \mathrm{f}[P_1(\boldsymbol{d}), P_2(\boldsymbol{d}), \ldots] \tag{2}$$

The goal is to find the optimal controller parameter $\boldsymbol{d}^*$ that minimizes the cost function J.

In most cases, Eq. (1) cannot be integrated analytically. Monte Carlo evaluation (MCE)[11] is a practical and flexible alternative to estimate the probabilities. The estimates of the probability and cost based on N samples are

$$\hat{P}(\boldsymbol{d}) = \frac{1}{N}\sum_{k=1}^{N} I[H(\boldsymbol{v}_k), C(\boldsymbol{d})] \tag{3}$$

$$\hat{J}(\boldsymbol{d}) = \mathrm{f}[\hat{P}_1(\boldsymbol{d}), \hat{P}_2(\boldsymbol{d}), \ldots] \tag{4}$$

The estimated cost $\hat{J}$ approaches the actual cost J in the limit as $N \to \infty$. For a finite N, because the probabilities defined are all binary variables, with the outcome of a trial taking one of two possible values (acceptable or unacceptable) for each MCE, the binomial test can be applied to determine exact confidence intervals for the estimates of the probabilities. Reference 2 provides the formula to compute the lower bound and upper bound of the confidence interval for the MCE corresponding to any specified confidence coefficients.

B. NDI

Dynamic inversion uses nonlinear full-state feedback to globally linearize dynamics of selected controlled variables. Linear controllers can then be designed to regulate these variables with desirable closed-loop dynamics.

Consider a nonlinear system with the same input and output dimensions,

$$\dot{\boldsymbol{x}} = \boldsymbol{f}(\boldsymbol{x}) + \boldsymbol{G}(\boldsymbol{x})\boldsymbol{u}, \qquad \boldsymbol{G}(\boldsymbol{x}) = [\boldsymbol{g}_1(x), \boldsymbol{g}_2(x), \ldots, \boldsymbol{g}_m(x)] \tag{5}$$

$$\boldsymbol{y} = \boldsymbol{h}(\boldsymbol{x}) \tag{6}$$

where $\boldsymbol{f}$ and $\boldsymbol{g}_j$ $(j = 1, 2, \ldots, m)$ are smooth vector fields on $\Re^n$, and $\boldsymbol{h}$ is a smooth function mapping $\Re^n \to \Re^m$. The inverse dynamics of Eqs. (5) and (6) are constructed by differentiating the individual elements of $\boldsymbol{y}$ a sufficient number of times until a term containing a control element appears.

Denote the Lie derivatives of the function h_i with respect to vector fields $\boldsymbol{f}$ and $\boldsymbol{g}_j$ as

$$L_f h_i = \frac{\partial h_i(\boldsymbol{x})}{\partial \boldsymbol{x}}\boldsymbol{f}(\boldsymbol{x}) \tag{7}$$

$$L_f^k h_i = L_f\left(L_f^{k-1} h_i\right) \tag{8}$$

and

$$L_{\boldsymbol{g}_j} h_i = \frac{\partial h_i(\boldsymbol{x})}{\partial \boldsymbol{x}}\boldsymbol{g}_j(\boldsymbol{x}) \tag{9}$$

For each h_i, define λ_i as the smallest integer such that at least one $j \in \{1, 2, \ldots, m\}$ satisfies

$$L_{\boldsymbol{g}_j}\left(L_f^{\lambda_i - 1} h_i\right) \neq 0 \tag{10}$$

Therefore, for the ith component of $\boldsymbol{y}$, we have

$$\dot{y}_i = L_f h_i + \sum_{j=1}^{m}\left(L_{\boldsymbol{g}_j} h_i\right)u_j = L_f h_i \tag{11}$$

$$\ddot{y}_i = L_f^2 h_i + \sum_{j=1}^{m} L_{\boldsymbol{g}_j}(L_f h_i)u_j = L_f^2 h_i \tag{12}$$

$$\vdots$$

$$y_i^{(\lambda_i)} = L_f^{\lambda_i} h_i + \sum_{j=1}^{m} L_{\boldsymbol{g}_j}\left(L_f^{\lambda_i - 1} h_i\right)u_j \tag{13}$$

After differentiating λ_i times of each output element y_i, the output dynamics can be represented as

$$\boldsymbol{y}^{[\lambda]} = \begin{bmatrix} y_1^{(\lambda_1)} \\ y_2^{(\lambda_2)} \\ \vdots \\ y_m^{(\lambda_m)} \end{bmatrix} = \begin{bmatrix} L_f^{\lambda_1} h_1 \\ L_f^{\lambda_2} h_2 \\ \vdots \\ L_f^{\lambda_m} h_m \end{bmatrix} + \begin{bmatrix} L_{\boldsymbol{g}_1} L_f^{\lambda_1 - 1} h_1 & L_{\boldsymbol{g}_2} L_f^{\lambda_1 - 1} h_1 & \cdots & L_{\boldsymbol{g}_m} L_f^{\lambda_1 - 1} h_1 \\ L_{\boldsymbol{g}_1} L_f^{\lambda_2 - 1} h_2 & L_{\boldsymbol{g}_2} L_f^{\lambda_2 - 1} h_2 & \cdots & L_{\boldsymbol{g}_m} L_f^{\lambda_2 - 1} h_2 \\ \cdots & \cdots & \cdots & \cdots \\ L_{\boldsymbol{g}_1} L_f^{\lambda_m - 1} h_m & L_{\boldsymbol{g}_2} L_f^{\lambda_m - 1} h_m & \cdots & L_{\boldsymbol{g}_m} L_f^{\lambda_m - 1} h_m \end{bmatrix}\boldsymbol{u} \tag{14}$$

or

$$\boldsymbol{y}^{[\lambda]} = \boldsymbol{f}^*(\boldsymbol{x}) + \boldsymbol{G}^*(\boldsymbol{x})\boldsymbol{u} \tag{15}$$

$\boldsymbol{\lambda} = (\lambda_1, \lambda_2, \ldots, \lambda_m)$ is called the vector relative degree at $\boldsymbol{x}_0$ if $L_{\boldsymbol{g}_j} L_f^k h_i(\boldsymbol{x}) = 0$, $0 \leq k \leq \lambda_i - 2$, for any $\boldsymbol{x}$ in the neighborhood of $\boldsymbol{x}_0$, and $\boldsymbol{G}^*(\boldsymbol{x}_0)$ is nonsingular. Define the feedback control law as

$$\boldsymbol{u} = -[\boldsymbol{G}^*(\boldsymbol{x})]^{-1}\boldsymbol{f}^*(\boldsymbol{x}) + [\boldsymbol{G}^*(\boldsymbol{x})]^{-1}\boldsymbol{v} \tag{16}$$

with $\boldsymbol{v}$ as the new control input. Then the output dynamics take the integrator-decoupled form

$$\boldsymbol{y}^{[\lambda]} = \boldsymbol{v} \tag{17}$$

Furthermore, if

$$\sum_{i=1}^{m} \lambda_i = n$$

the nonlinear coordinate transformation $\boldsymbol{\varsigma} = T(\boldsymbol{x})$ can be chosen such that the original system, Eqs. (5) and (6), is linearized exactly:

$$\begin{aligned} \varsigma_1^i &= h_i \\ \varsigma_2^i &= L_f h_i \\ &\vdots \\ \varsigma_{\gamma_i}^i &= L_f^{\lambda_i - 1} h_i \end{aligned} \tag{18}$$

where $i = 1, 2, \ldots, m$. We state the dynamic equations of the transformed system in canonical form,

$$\begin{aligned} \dot{\varsigma}_1^i &= \varsigma_2^i \\ \dot{\varsigma}_2^i &= \varsigma_3^i \\ &\vdots \\ \dot{\varsigma}_{\lambda_i}^i &= L_f^{\lambda_i} h_i + \sum_{j=1}^{m} L_{\boldsymbol{g}_j}\left(L_f^{\lambda_i - 1} h_i\right)u_j = \boldsymbol{v}_i \end{aligned} \tag{19}$$

where $i = 1, 2, \ldots, m$. For the decoupled linear systems, Eq. (19), we can design each v_i, $i = 1, 2, \ldots, m$, separately, combining all of them in Eq. (16) to give the nonlinear control law $\boldsymbol{u}$.

Note that $\boldsymbol{G}^*(\cdot)$ needs to be nonsingular for vector relative degree to be well defined. If this is not the case, the system can be dynamically extended by adding integrators to certain input channels, producing a well-defined vector relative degree.[8] In this paper, integrators have been added to the engine throttle setting to ensure that the vector relative degree is well defined.

If

$$\sum_{i=1}^{m} \lambda_i < n$$

Eq. (18) quantifies only a partial set of coordinates for transformation. In that case, stability of the system, Eqs. (5) and (6), depends

not only on the output dynamics, Eq. (17), but also on the stability of zero dynamics, as noted in Ref. 8. For our application

$$\sum_{i=1}^{m} \lambda_i = n$$

and there are no zero dynamics.

III. Mathematical Model of a Hypersonic Aircraft

Consider the longitudinal flight control of a hypersonic aircraft cruising at a Mach number of 15 and at an altitude of 110,000 ft (Refs. 7 and 12). The dynamic equations are

$$\dot{V} = (T\cos\alpha - D)/m - \mu\sin\gamma/r^2 \tag{20}$$

$$\dot{\gamma} = (L + T\sin\alpha)/(mV) - [(\mu - V^2 r)\cos\gamma]/(Vr^2) \tag{21}$$

$$\dot{h} = V\sin\gamma \tag{22}$$

$$\dot{\alpha} = q - \dot{\gamma} \tag{23}$$

$$\dot{q} = M_{yy}/I_{yy} \tag{24}$$

where

$$L = \tfrac{1}{2}\rho V^2 S C_L \tag{25}$$

$$D = \tfrac{1}{2}\rho V^2 S C_D \tag{26}$$

$$T = \tfrac{1}{2}\rho V^2 S C_T \tag{27}$$

The thrust coefficient C_T is a function of throttle setting δT:

$$C_T = \begin{cases} \nu_{16}0.0105\left[1 - \nu_{17}164(\alpha - \alpha_0)^2\right](1 + \nu_{18}17/M)(1 + \nu_{19}0.15)\delta T & \text{if} \quad \delta T < 1 \\ \nu_{16}0.0105\left[1 - \nu_{17}164(\alpha - \alpha_0)^2\right](1 + \nu_{18}17/M)(1 + \nu_{19}0.15\delta T) & \text{if} \quad \delta T \geq 1 \end{cases} \tag{28}$$

where α_0 takes the trim value 0.0315 rad and

$$M_{yy} = \tfrac{1}{2}\rho V^2 S\bar{c}[C_M(\alpha) + C_M(\delta E) + C_M(q)] \tag{29}$$

$$r = h + R_E \tag{30}$$

The aerodynamic coefficients and inertial data are given in Appendix A. Interpolation by lookup tables or spline fits could be used for precise simulation. We have used relatively simple functions to fit the data around the nominal cruising condition. Here, 28 inertial and aerodynamic parameters (identified in Appendix A) are assumed to be uncertain. Each parameter is multiplied by an element of the uncertainty vector $\boldsymbol{\nu}$ that is assumed to follow a normal distribution with a mean of 1 and a standard deviation of 0.1. At the trimmed cruise condition ($M = 15$, $V = 15{,}060$ ft/s, $h = 110{,}000$ ft, $\alpha = 0.0315$ rad, $\delta T = 0.183$, $\delta E = -0.0066$ rad, and $T = 4.6853 \times 10^4$ lbf), a linearized model of the nominal open-loop dynamics has eigenvalues of $-0.8, 0.687, -0.0001 \pm 0.0263j$, and 0.0008. The first two eigenvalues represent a statically unstable short-period mode, the complex pair of eigenvalues portrays a lightly damped phugoid mode, and the last real eigenvalue indicates a mildly unstable height mode. Consequently, cruising flight would be subject to attitude and height divergence that would require stabilizing feedback control.

IV. Stability and Performance Metrics

Three aspects of flight control robustness are of concern in this design: stability, performance in velocity command response, and performance in altitude command response. The command responses are initiated at the trimmed condition. State histories of the aircraft's nonlinear response to the velocity and altitude commands are evaluated for stability and performance. Table 1 lists 39 stability and performance metrics that characterize the responses to a step velocity command change of 100 ft/s and a step altitude command change of 2000 ft. The indicator functions with subscripts V and h denote the metrics for velocity and altitude command responses.

The cost function chosen to guide the design is a weighted quadratic sum of the 39 probabilities of design requirement violation:

$$J = \sum_{j=1}^{39} w_j P_j^2 \tag{31}$$

As indicated in Table 1, the stability weight w_1 is chosen as 10, the weight for each less-demanding performance metric is selected as 1, and the weight for each more-demanding performance metric is 0.1.

V. Stochastic Robust NDI Control Law

First, we consider the nominal dynamics of the hypersonic aircraft with velocity and altitude commands:

$$\boldsymbol{y}_{\text{com}} = \begin{pmatrix} V \\ h \end{pmatrix} \tag{32}$$

Table 1 Stability and performance metrics for a hypersonic aircraft

Metric number	Weight in J	Indicator function	Design requirement
1	10.0	I_i	System stability
2 (3)	0.1 (1.0)	$I_{V,Ts25}$ ($I_{V,Ts50}$)	10% settling time less than 25 s (50 s)
4 (5)	0.1 (1.0)	$I_{V,R25}$ ($I_{V,R50}$)	90% rise time less than 25 s (50 s)
6	0.1	$I_{V,\text{Re}v}$	No reversal of response in V before peaking
7 (8)	0.1 (1.0)	$I_{V,D5}$ ($I_{V,D10}$)	10% dwell time less than 5 s (10 s)
9 (10)	0.1 (1.0)	$I_{V,OS10}$ ($I_{V,OS20}$)	Overshoot less than 10% (20%)
11 (12)	0.1 (1.0)	$I_{V,\Delta\alpha 0.5}$ ($I_{V,\Delta\alpha 1}$)	Maximum change in α less than 0.5 deg (1 deg)
13 (14)	0.1 (1.0)	$I_{V,g1}$ ($I_{V,g2}$)	Maximum load factor less than 1 g (2 g)
15 (16)	0.1 (1.0)	$I_{V,\Delta h0.25}$ ($I_{V,\Delta h0.5}$)	Maximum change of h less than 0.25% (0.5%)
17 (18)	0.1 (1.0)	$I_{V,\delta T50}$ ($I_{V,\delta T100}$)	Maximum change in thrust less than 50% (100%)
19 (20)	0.1 (1.0)	$I_{V,\delta E5}$ ($I_{V,\delta E10}$)	Maximum change in δE less than 5 deg (10 deg)
21 (22)	0.1 (1.0)	$I_{h,Ts50}$ ($I_{h,Ts100}$)	10% settling time less than 50 s (100 s)
23 (24)	0.1 (1.0)	$I_{h,R50}$ ($I_{h,R100}$)	90% rise time less than 50 s (100 s)
25	0.1	$I_{h,\text{Re}v}$	No reversal of response in h before peaking
26 (27)	0.1 (1.0)	$I_{h,D10}$ ($I_{h,D20}$)	10% dwell time less than 10 s (20 s)
28 (29)	0.1 (1.0)	$I_{h,OS20}$ ($I_{h,OS40}$)	Overshoot less than 20% (40%)
30 (31)	0.1 (1.0)	$I_{h,\Delta\alpha 0.5}$ ($I_{h,\Delta\alpha 1}$)	Maximum change in α less than 0.5 deg (1 deg)
32 (33)	0.1 (1.0)	$I_{h,g1}$ ($I_{h,g2}$)	Maximum load factor less than 1 g (2 g)
34 (35)	0.1 (1.0)	$I_{h,\Delta V0.25}$ ($I_{h,\Delta V0.5}$)	Maximum change of V less than 0.25% (0.5%)
36 (37)	0.1 (1.0)	$I_{h,\delta T50}$ ($I_{h,\delta T100}$)	Maximum change in thrust less than 50% (100%)
38 (39)	0.1 (1.0)	$I_{h,\delta E5}$ ($I_{h,\delta E10}$)	Maximum change in δE less than 5 deg (10 deg)

Integral compensation is used to minimize the steady-state error of the command response; hence,

$$V_I = \int_0^t [V(\tau) - V^*]\,\mathrm{d}\tau \tag{33}$$

and

$$h_I = \int_0^t [h(\tau) - h^*]\,\mathrm{d}\tau \tag{34}$$

where V^* and h^* are the commanded values.

In this control example, dynamic extension ensures that the vector relative degree is well defined. We assume that engine dynamics take a second-order form,

$$\ddot{\delta T} = k_1 \delta T + k_2 \dot{\delta T} + k_3 \delta T_{\mathrm{com}} \tag{35}$$

where choosing $k_1 = k_2 = 0$ and $k_3 = 1$ provides a suitable model.

By augmenting the state variables as

$$\boldsymbol{x}_1 = \begin{bmatrix} V_I \\ V \\ \gamma \end{bmatrix}, \qquad \boldsymbol{x}_2 = \begin{bmatrix} \delta T \\ h_I \\ h \\ \alpha \end{bmatrix}, \qquad \boldsymbol{x}_3 = \begin{pmatrix} \dot{\delta T} \\ q \end{pmatrix} \tag{36}$$

and defining the control vector as

$$\boldsymbol{u} = \begin{pmatrix} \dot{\delta T}_{\mathrm{com}} \\ \delta E \end{pmatrix} \tag{37}$$

the aircraft equations of motion can be put into a triangular form,

$$\begin{aligned} \dot{\boldsymbol{x}}_1 &= \boldsymbol{f}_1(\boldsymbol{x}_1, \boldsymbol{x}_2), \qquad \dot{\boldsymbol{x}}_2 = \boldsymbol{f}_2(\boldsymbol{x}_1, \boldsymbol{x}_2, \boldsymbol{x}_3) \\ \dot{\boldsymbol{x}}_3 &= \boldsymbol{f}_3(\boldsymbol{x}_1, \boldsymbol{x}_2, \boldsymbol{x}_3) + \boldsymbol{G}_3(\boldsymbol{x}_1, \boldsymbol{x}_2, \boldsymbol{x}_3)\boldsymbol{u} \end{aligned} \tag{38}$$

The output dynamic equation (15) is derived by differentiating V three times and h four times. Using the notation

$$\boldsymbol{z}^T = [V \quad \gamma \quad \alpha \quad \delta T \quad h] \tag{39}$$

we have

$$\begin{aligned} \dot{V} &= (T\cos\alpha - D)/m - \mu \sin\gamma / r^2 \\ \ddot{V} &= (1/m)\omega_1 \dot{\boldsymbol{z}}, \qquad \dddot{V} = (1/m)\left(\omega_1 \ddot{\boldsymbol{z}} + \dot{\boldsymbol{z}}^T \Omega_2 \dot{\boldsymbol{z}}\right) \end{aligned} \tag{40}$$

and

$$\begin{aligned} \dot{h} &= V\sin\gamma, \qquad \ddot{h} = \dot{V}\sin\gamma + V\dot{\gamma}\cos\gamma \\ \dddot{h} &= \ddot{V}\sin\gamma + 2\dot{V}\dot{\gamma}\cos\gamma - V\dot{\gamma}^2\sin\gamma + V\ddot{\gamma}\cos\gamma \\ h^{(4)} &= \dddot{V}\sin\gamma + 3\ddot{V}\dot{\gamma}\cos\gamma - 3\dot{V}\dot{\gamma}^2\sin\gamma + 3\dot{V}\ddot{\gamma}\cos\gamma \\ &\quad - 3V\dot{\gamma}\ddot{\gamma}\sin\gamma - V\dot{\gamma}^3\cos\gamma + V\dddot{\gamma}\cos\gamma \end{aligned} \tag{41}$$

where

$$\ddot{\gamma} = \pi_1 \dot{\boldsymbol{z}}, \qquad \dddot{\gamma} = \pi_1 \ddot{\boldsymbol{z}} + \dot{\boldsymbol{z}}^T \Xi_2 \dot{\boldsymbol{z}} \tag{42}$$

The vectors ω_1, π_1 and matrices Ω_2, Ξ_2 are given in Appendix B.

From Eq. (39), we have $\ddot{\boldsymbol{z}}^T = [\dddot{V} \quad \ddot{\gamma} \quad \dddot{\alpha} \quad \ddot{\delta T} \quad \dddot{h}]$. In terms of Eqs. (23), (24), and (35), we separate the second derivatives of angle of attack α and throttle setting δT into control-independent and control-dependent parts:

$$\dddot{\alpha} = \dddot{\alpha}_0 + \dddot{\alpha}_{\delta E}\delta E \tag{43}$$

$$\ddot{\delta T} = \ddot{\delta T}_0 + \ddot{\delta T}_{\mathrm{com}}\delta T_{\mathrm{com}} \tag{44}$$

where $\dddot{\alpha}_{\delta E}$ represents the first derivative of $\dddot{\alpha}$ with respect to δE, and $\ddot{\delta T}_{\mathrm{com}}$ represents the first derivative of $\ddot{\delta T}$ with respect to δT_{com}. Therefore, $\ddot{\boldsymbol{z}}$ can be written as

$$\begin{aligned} \ddot{\boldsymbol{z}}^T &= [\dddot{V} \quad \ddot{\gamma} \quad \dddot{\alpha}_0 \quad \ddot{\delta T}_0 \quad \dddot{h}] \\ &\quad + [\delta T_{\mathrm{com}} \quad \delta E] \cdot \begin{pmatrix} 0 & 0 & 0 & \ddot{\delta T}_{\mathrm{com}} & 0 \\ 0 & 0 & \dddot{\alpha}_{\delta E} & 0 & 0 \end{pmatrix} = \ddot{\boldsymbol{z}}_0^T + \boldsymbol{u}^T \ddot{\boldsymbol{z}}_u^T \end{aligned} \tag{45}$$

By Eqs. (40) and (41), the output dynamic equation can be written as

$$\begin{pmatrix} \dddot{V} \\ h^{(4)} \end{pmatrix} = \boldsymbol{f}^*(\boldsymbol{x}) + \boldsymbol{G}^*(\boldsymbol{x})\boldsymbol{u} \tag{46}$$

where

$$\boldsymbol{f}^* = \begin{bmatrix} (1/m)\omega_1 \ddot{\boldsymbol{z}}_0 + (1/m)\dot{\boldsymbol{z}}^T \Omega_2 \dot{\boldsymbol{z}} \\ 3\ddot{V}\dot{\gamma}\cos\gamma - 3\dot{V}\dot{\gamma}^2\sin\gamma + 3\dot{V}\ddot{\gamma}\cos\gamma - 3V\dot{\gamma}\ddot{\gamma}\sin\gamma - V\dot{\gamma}^3\cos\gamma + \left[(1/m)\omega_1 \ddot{\boldsymbol{z}}_0 + (1/m)\dot{\boldsymbol{z}}^T \Omega_2 \dot{\boldsymbol{z}}\right]\sin\gamma + V\cos\gamma\left(\pi_1 \ddot{\boldsymbol{z}}_0 + \dot{\boldsymbol{z}}^T \Pi_2 \dot{\boldsymbol{z}}\right) \end{bmatrix} \tag{47}$$

$$\boldsymbol{G}^* = \begin{pmatrix} (T_{\delta T}\cos\alpha/m)\dot{\delta T}_{\mathrm{com}} & [(T_\alpha \cos\alpha - T\sin\alpha - D_\alpha)/m]\dddot{\alpha}_{\delta E} \\ [T_{\delta T}\sin(\alpha+\gamma)/m]\dot{\delta T}_{\mathrm{com}} & \{[T\cos(\alpha+\gamma) + T_\alpha \sin(\alpha+\gamma) + L_\alpha \cos\gamma - D_\alpha \sin\gamma]/m\}\dddot{\alpha}_{\delta E} \end{pmatrix} \tag{48}$$

The determinant of $\boldsymbol{G}^*$ is

$$\det(\boldsymbol{G}^*) = \left(T_{\delta T}\ddot{\delta T}_{\mathrm{com}}\dddot{\alpha}_{\delta E} \mid m^2\right)\cos\gamma(T + L_\alpha \cos\alpha + D_\alpha \sin\alpha) \tag{49}$$

where L_α, D_α, and T_α denote the partial derivatives of L, D, and T with respect to the angle of attack α and $T_{\delta T}$ denotes the partial derivative of T with respect to the throttle setting δT. The nonsingular condition for $\boldsymbol{G}^*$ can be represented as

$$\det(\boldsymbol{G}^*) \neq 0 \Leftrightarrow (T + L_\alpha \cos\alpha + D_\alpha \sin\alpha)\cos\gamma \neq 0 \tag{50}$$

Therefore, $\boldsymbol{G}^*$ is nonsingular unless the flight path is vertical or $(T + L_\alpha \cos\alpha + D_\alpha \sin\alpha) = 0$. If $\boldsymbol{G}^*$ is nonsingular and $\boldsymbol{u}$ is chosen as Eq. (16), the output dynamics can be written in decoupled-integrator form

$$\begin{pmatrix} V^{(3)} \\ h^{(4)} \end{pmatrix} = \begin{pmatrix} v_1 \\ v_2 \end{pmatrix} \tag{51}$$

By assuming desired command rates as zero, and using Eqs. (40) and (41), we define a nonlinear coordinate transformation, $\xi = T_1(\boldsymbol{x}, V^*)$ and $\eta = T_2(\boldsymbol{x}, h^*)$, as

$$\begin{aligned} \xi_1 &= \int_0^t [V(\tau) - V^*]\,\mathrm{d}\tau, \qquad \xi_2 = V - V^* \\ \xi_3 &= \dot{V}, \qquad \xi_4 = \ddot{V} \end{aligned}$$

and

$$\begin{aligned} \eta_1 &= \int_0^t [h(\tau) - h^*]\,\mathrm{d}\tau, \qquad \eta_2 = h - h^* \\ \eta_3 &= \dot{h}, \qquad \eta_4 = \ddot{h}, \qquad \eta_5 = \dddot{h} \end{aligned} \tag{52}$$

This results in decoupled subsystems

$$\dot{\boldsymbol{\xi}} = \boldsymbol{A}_1 \boldsymbol{\xi} + \boldsymbol{b}_1 v_1 \tag{53}$$

where

$$\boldsymbol{A}_1 = \begin{bmatrix} 0 & 1 & 0 & 0 \\ 0 & 0 & 1 & 0 \\ 0 & 0 & 0 & 1 \\ 0 & 0 & 0 & 0 \end{bmatrix}, \qquad \boldsymbol{b}_1 = \begin{bmatrix} 0 \\ 0 \\ 0 \\ 1 \end{bmatrix} \tag{54}$$

and

$$\dot{\boldsymbol{\eta}} = \boldsymbol{A}_2\boldsymbol{\eta} + \boldsymbol{b}_2 v_2 \tag{55}$$

where

$$\boldsymbol{A}_2 = \begin{bmatrix} 0 & 1 & 0 & 0 & 0 \\ 0 & 0 & 1 & 0 & 0 \\ 0 & 0 & 0 & 1 & 0 \\ 0 & 0 & 0 & 0 & 1 \\ 0 & 0 & 0 & 0 & 0 \end{bmatrix}, \qquad \boldsymbol{b}_2 = \begin{bmatrix} 0 \\ 0 \\ 0 \\ 0 \\ 1 \end{bmatrix} \tag{56}$$

For the transformed linear systems, Eqs. (53) and (55), we design the new inputs v_1 and v_2 as linear-quadratic control laws. Considering intermediate objective functions

$$J_1 = \int_0^\infty \left(\boldsymbol{\xi}^T \boldsymbol{Q}_1 \boldsymbol{\xi} + r_1 v_1^2\right) \mathrm{d}t \tag{57}$$

and

$$J_2 = \int_0^\infty \left(\boldsymbol{\eta}^T \boldsymbol{Q}_2 \boldsymbol{\eta} + r_2 v_2^2\right) \mathrm{d}t \tag{58}$$

the new input v_1 is derived by minimizing J_1 subject to Eq. (53):

$$v_1 = -r_1^{-1} \boldsymbol{b}_1^T \boldsymbol{P}_1 \boldsymbol{\xi} \tag{59}$$

$\boldsymbol{P}_1$ is the positive-definite solution to the Riccati equation with design parameters $\boldsymbol{Q}_1$ and r_1,

$$\boldsymbol{A}_1^T \boldsymbol{P}_1 + \boldsymbol{P}_1 \boldsymbol{A}_1 - r_1^{-1} \boldsymbol{P}_1 \boldsymbol{b}_1 \boldsymbol{b}_1^T \boldsymbol{P}_1 + \boldsymbol{Q}_1 = 0, \qquad (\boldsymbol{Q}_1, r_1 > 0) \tag{60}$$

Similarly, minimizing J_2 subject to Eq. (55) gives

$$v_2 = -r_2^{-1} \boldsymbol{b}_2^T \boldsymbol{P}_2 \boldsymbol{\eta} \tag{61}$$

$\boldsymbol{P}_2$ is the positive-definite solution to the Riccati equation with design parameters $\boldsymbol{Q}_2$ and r_2,

$$\boldsymbol{A}_2^T \boldsymbol{P}_2 + \boldsymbol{P}_2 \boldsymbol{A}_2 - r_2^{-1} \boldsymbol{P}_2 \boldsymbol{b}_2 \boldsymbol{b}_2^T \boldsymbol{P}_2 + \boldsymbol{Q}_2 = 0, \qquad (\boldsymbol{Q}_2, r_2 > 0) \tag{62}$$

The nonlinear control law $\boldsymbol{u}$ is obtained by inserting $\boldsymbol{v} = [v_1 \;\; v_2]^T$ into Eq. (16):

$$\boldsymbol{u} = -[\boldsymbol{G}^*(\boldsymbol{x})]^{-1} \boldsymbol{f}^*(\boldsymbol{x}) + [\boldsymbol{G}^*(\boldsymbol{x})]^{-1} \begin{pmatrix} -r_1 \boldsymbol{b}_1^T \boldsymbol{P}_1 \boldsymbol{\xi} \\ -r_2 \boldsymbol{b}_2^T \boldsymbol{P}_2 \boldsymbol{\eta} \end{pmatrix} \tag{63}$$

Figure 1 illustrates the structure of this NDI control law.

Considering the system robustness subject to the variations of the uncertain aerodynamic parameters defined in Appendix A, appropriate $\boldsymbol{Q}_1$, r_1, $\boldsymbol{Q}_2$, and r_2 in the intermediate objective functions are found by minimizing the stochastic robustness cost function [Eq. (31)]. For simplicity, we choose the design parameters $\boldsymbol{Q}_1 = \mathrm{diag}\{q_1, q_2, q_3, q_4\}$ and $\boldsymbol{Q}_2 = \mathrm{diag}\{q_5, q_6, q_7, q_8, q_9\}$, and the design parameter vector is

$$\boldsymbol{d} = \{q_1, q_2, \ldots, q_9, r_1, r_2\} \tag{64}$$

Satisfactory values of the eleven design parameters in Eq. (64) are computed by applying a genetic algorithm (GA) to a Monte Carlo simulation of the hypersonic aircraft, which is based on Eqs. (20–30) and the uncertainty models contained in Appendix A. The discrepancy between the Monte Carlo estimate and the true value results in apparent noise in the evaluation of the cost function. Furthermore, the cost function is multimodal, having large plateau areas and corners, and so traditional gradient-based search algorithms can become stuck in local minima and cannot escape from large plateau areas in the cost function.

The GA[13] is a randomized global optimization method that deals with the design parameter vectors as though they are the chromosomes of biological organisms that are competing for survival. Each element in the design parameter vector is represented by a binary number sequence, and the elements are concatenated to compose a single chromosome. There are four operations in each generation of the chromosome evolution: evaluation, selection, crossover, and mutation. The initial population is formed by randomly generating a number of chromosomes. The fitness of each chromosome is evaluated by Monte Carlo simulation, and high-fitness chromosomes are selected to survive to the next generation. Chromosomes with lower cost J have higher fitness. The selected chromosomes are paired randomly and subjected to crossover, in which the tails of a pair of chromosomes are swapped at a random point along the binary sequence with probability ranging from 0.6 to 1. After crossover, the binary number sequence in each chromosome may be mutated with some very low probability (usually less than 0.1). Mutation, in which a binary number of the chromosome is flipped from 0 to 1 or from 1 to 0, allows the algorithm to continue considering parameter vectors throughout the design space, even as the algorithm is converging to a high-fitness design vector.

VI. Results and Stochastic Robustness Analysis of Final Design

The design parameter vector Eq. (64), found by the genetic algorithm after 20 generations, is given as

$$\boldsymbol{d} = \{8.54 \times 10^{-6}, 0.34, 0.86, 47.93, 1.1 \times 10^{-11}, 2.35 \times 10^{-3},$$
$$0.52, 220.6, 57.12, 0.89, 1.05\} \tag{65}$$

The performance for the nominal closed-loop system is shown in Figs. 2 and 3. Figure 2 shows the response due to a 100-ft/s step-velocity command from the trimmed condition ($V = 15{,}060$ ft/s, $h = 110{,}000$ ft). The velocity converges to the command value in 30 s with little change in altitude and with a change of angle of attack of less than 0.06 deg. Note that the use of thrust is unrealistically high, as there are limits to the thrust available. The example will be rerun with revised design weights in the future. Nevertheless, the example illustrates the effectiveness of the design approach for the specified criteria. Figure 3 shows the velocity, altitude change, and control input time histories to a 2000-ft step-altitude command. The altitude converges to the command value in 75 s, with a change of angle of attack of less than 0.5 deg. Figures 2 and 3 demonstrate that the nominal system has good performance.

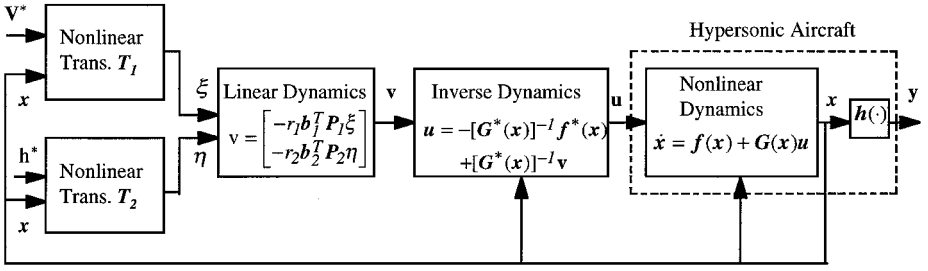

Fig. 1 NDI control law structure.

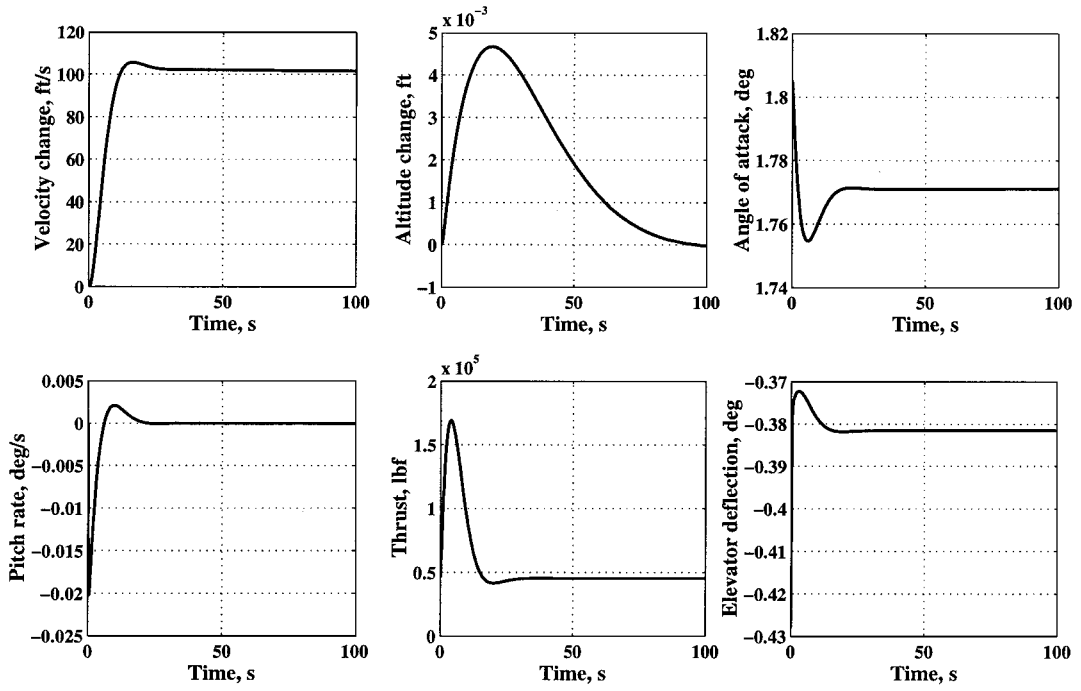

Fig. 2 Response with NDI controller to a 100-ft/s step-velocity command.

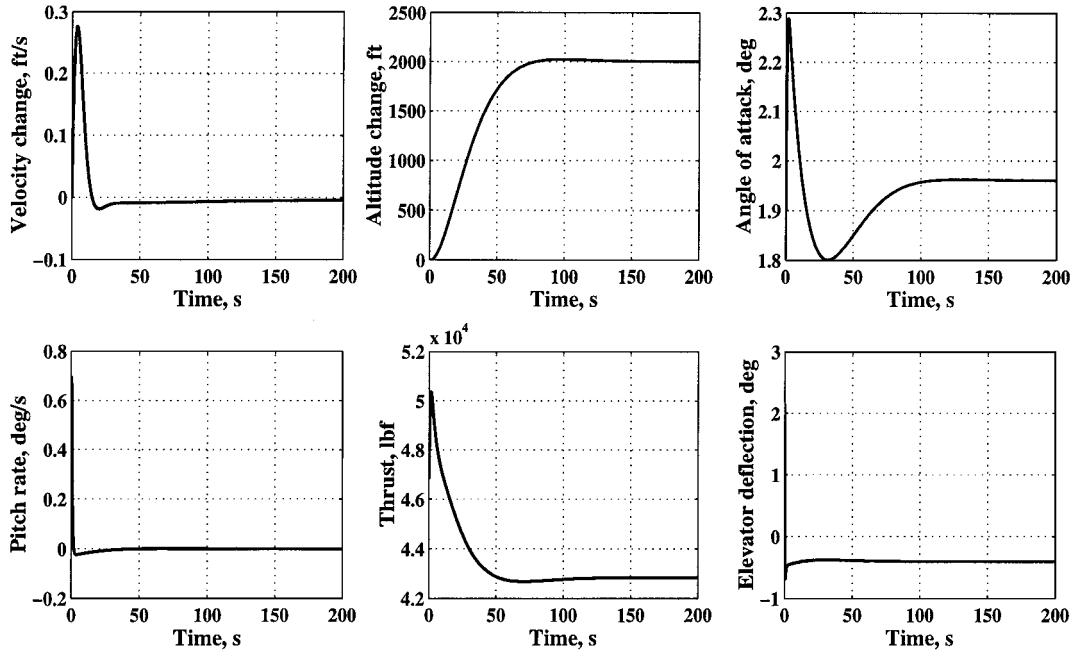

Fig. 3 Response with NDI controller to a 2000-ft step-altitude command.

Two thousand MCEs of the control design with the controller parameter presented in Eq. (65) show that the cost, Eq. (31), of NDI equals 1.23 compared to 1.72 for LQ.[7] The closed-loop probability of instability of NDI equals zero with a 95% confidence interval of (0, 0.0018). Figure 4 shows the robustness profiles of this nonlinear design NDI compared to the robustness profiles of the linear design LQ. As indicated in Table 1, metric 1 represents the probability of instability, metrics 2–20 represent the 19 performance metrics defined for velocity command response, and metrics 21–39 represent the performance metrics for altitude command response. Figure 4 shows that the NDI design has 5–56% lower probability of exceeding settling time than the LQ design (metrics 2, 3, 21, and 22), 15–80% lower probability of exceeding rise time (metrics 4, 5, 23, and 24), and 10–90% lower probability of exceeding dwell time (metrics 7, 8, 26, and 27). The NDI design has also reduced the probability of load factor exceedance by more than 80% compared to the LQ design (metrics 13, 14, 32, and 33).

However, NDI has larger probability of control effort exceedance corresponding to metric 18, $I_{V,\delta T100}$, and metric 36, $I_{h,\delta T50}$, due to the possibility that NDI may cancel some useful nonlinearities. Furthermore, in Eqs. (57) and (58), the weights r_1 and r_2 penalize large inputs v_1 and v_2 instead of penalizing thrust directly as in LQ. We can see that NDI performs better than LQ in metric 19 (20), $I_{V,\delta E5}$ ($I_{V,\delta E10}$), and metric 38 (39), $I_{h,\delta E5}$ ($I_{h,\delta E10}$). The robustness profiles can be adjusted by changing the weights in the robustness cost function. For example, tradeoffs between using less thrust and accepting longer rise time or putting heavy weight on $P_{h,Ts}$ to decrease the probability of settling time exceedance are examined easily. The NDI controller will be demonstrated over the entire flight envelope in future work, illustrating the value of this nonlinear approach.

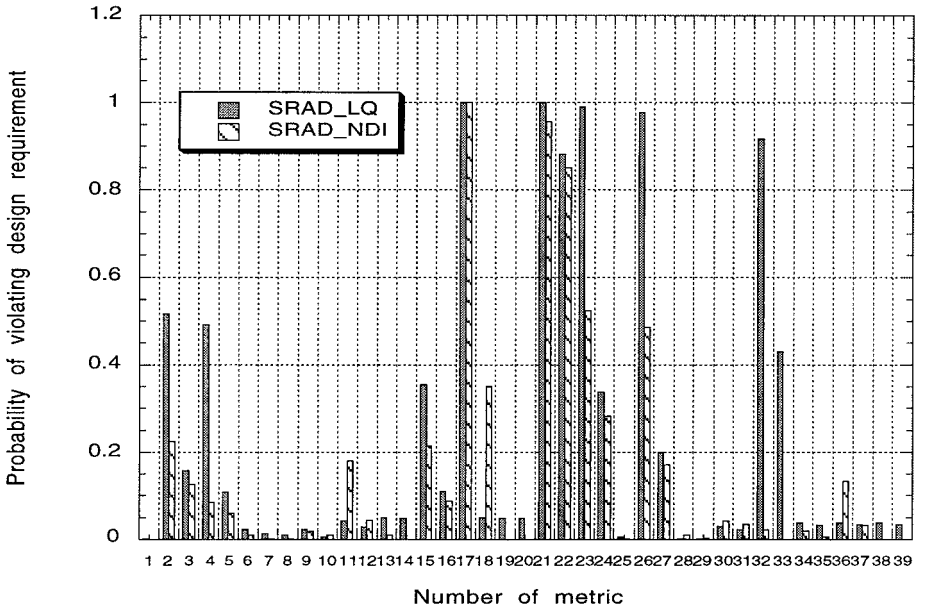

Fig. 4 Comparison of the robustness profiles of the stochastic robust control based on LQ regulator and NDI structure.

VII. Conclusions

In this paper, we have designed robust nonlinear control laws for a hypersonic aircraft that combine the elegance of NDI, which is valid over the entire flight envelope, with the directness and flexibility of MCE and numerical search. This combination allows the NDI to be robust to uncertain parameters. The example considered in this paper has 39 stability and performance design requirements and is subject to 28 uncertain system parameters. Other robust synthesis methods would find such a design formidable, whereas the stochastic robust nonlinear control design given in this paper shows good performance and robustness profiles. It has reduced design cost by 30% compared to the LQ design. The method should find widespread practical application because it is well matched to fulfilling design requirements that are expressed in conventional engineering terms, and it makes full use of the information contained in high-fidelity system models and simulations. As a simulation-based method for design and analysis, it directly addresses central issues for control system certification.

Appendix A: Aerodynamic Coefficients and Atmospheric Model

The aerodynamic coefficients are fitted to the data around the nominal cruising condition. Here, 28 inertial and aerodynamic parameters are assumed to be uncertain, with ν_i $(i = 1, 2, \ldots, 28)$ denoting an element of the uncertainty vector $\boldsymbol{\nu}$:

$$m = \nu_1 m_0 \tag{A1}$$

$$I_{yy} = \nu_2 I_0 \tag{A2}$$

$$S = \nu_3 S_0 \tag{A3}$$

$$\bar{c} = \nu_4 \bar{c}_0 \tag{A4}$$

$$a = \nu_5\left(\nu_6 8.99 \times 10^{-9} h^2 - \nu_7 9.16 \times 10^{-4} h + 996\right) \tag{A5}$$

$$M = V/a \tag{A6}$$

$$\rho = 0.00238 e^{-h/\nu_8 24000} \tag{A7}$$

$$C_L = \nu_9 \alpha(0.493 + \nu_{10} 1.91/M) \tag{A8}$$

$$C_D = \nu_{11} 0.0082\left(\nu_{12} 171\alpha^2 + \nu_{13} 1.15\alpha + 1\right) \times \left(\nu_{14} 0.0012M^2 - \nu_{15} 0.054M + 1\right) \tag{A9}$$

$$C_T = \begin{cases} \nu_{16} 0.0105\left[1 - \nu_{17} 164(\alpha - \alpha_0)^2\right](1 + \nu_{18} 17/M)(1 + \nu_{19} 0.15)\delta T & \text{if} \quad \delta T < 1 \\ \nu_{16} 0.0105\left[1 - \nu_{17} 164(\alpha - \alpha_0)^2\right](1 + \nu_{18} 17/M)(1 + \nu_{19} 0.15\delta T) & \text{if} \quad \delta T \geq 1 \end{cases} \tag{A10}$$

where α_0 takes the trim value 0.0315 rad.

$$C_M(\alpha) = \nu_{20} 10^{-4}(0.06 - e^{-\nu_{21} M/3}) \times \left(-\nu_{22} 6565\alpha^2 + \nu_{23} 6875\alpha + 1\right) \tag{A11}$$

$$C_M(q) = (\bar{c}/2V) q \nu_{24}(-\nu_{25} 0.025M + 1.37) \times \left(-\nu_{26} 6.83\alpha^2 + \nu_{27} 0.303\alpha - 0.23\right) \tag{A12}$$

$$C_M(\delta E) = \nu_{28} 0.0292(\delta E - \alpha) \tag{A13}$$

Appendix B: Command Variable Derivatives

The vectors $\boldsymbol{\omega}_1$, $\boldsymbol{\pi}_1$, and matrices Ω_2, Ξ_2 in the differentiation of the command variables V and h are given hereafter. L_V, L_α, and L_h denote the first-order derivatives of the lift with respect to the velocity, angle of attack, and altitude; L_{VV}, $L_{V\alpha}$, $L_{\alpha\alpha}$, ..., denote the second-order derivatives. Derivatives for drag D and thrust T are represented in the same way:

$$\omega_1^T = \begin{bmatrix} T_V \cos\alpha - D_V \\ -m\mu \cos\gamma / r^2 \\ T_\alpha \cos\alpha - T \sin\alpha - D_\alpha \\ T_{\delta T} \cos\alpha \\ T_h \cos\alpha - D_h + (2m\mu \sin\gamma / r^3) r_h \end{bmatrix} \tag{B1}$$

$$\Omega_2 = [\omega_{21} \quad \omega_{22} \quad \omega_{23} \quad \omega_{24} \quad \omega_{25}] \tag{B2}$$

where

$$\omega_{21} = \begin{bmatrix} T_{VV}\cos\alpha - D_{VV} \\ 0 \\ T_{V\alpha}\cos\alpha - T_V\sin\alpha - D_{V\alpha} \\ T_{V\delta T}\cos\alpha \\ T_{Vh}\cos\alpha - D_{Vh} \end{bmatrix} \tag{B3}$$

$$\omega_{22} = \begin{bmatrix} 0 \\ m\mu\sin\gamma/r^2 \\ 0 \\ 0 \\ (2m\mu\cos\gamma/r^3)r_h \end{bmatrix} \tag{B4}$$

$$\omega_{23} = \begin{bmatrix} T_{V\alpha}\cos\alpha - T_V\sin\alpha - D_{V\alpha} \\ 0 \\ T_{\alpha\alpha}\cos\alpha - 2T_\alpha\sin\alpha - T\cos\alpha - D_{\alpha\alpha} \\ T_{\alpha\delta T}\cos\alpha - T_{\delta T}\sin\alpha \\ T_{\alpha h}\cos\alpha - T_h\sin\alpha - D_{\alpha h} \end{bmatrix} \tag{B5}$$

$$\omega_{24} = \begin{bmatrix} T_{V\delta T}\cos\alpha \\ 0 \\ T_{\alpha\delta T}\cos\alpha - T_{\delta T}\sin\alpha \\ T_{\delta T\delta T}\cos\alpha \\ T_{\delta Th}\cos\alpha \end{bmatrix} \tag{B6}$$

$$\omega_{25} = \begin{bmatrix} T_{Vh}\cos\alpha - D_{Vh} \\ (2m\mu\cos\gamma/r^3)r_h \\ T_{\alpha h}\cos\alpha - T_h\sin\alpha - D_{\alpha h} \\ T_{\delta Th}\cos\alpha \\ T_{hh}\cos\alpha - D_{hh} - (6m\mu\sin\gamma/r^4)r_h^2 \end{bmatrix} \tag{B7}$$

$$\pi_1^T = \begin{bmatrix} \dfrac{L_V + T_V\sin\alpha}{mV} - \dfrac{L + T\sin\alpha}{mV^2} + \dfrac{\mu\cos\gamma}{V^2r^2} + \dfrac{\cos\gamma}{r} \\ \dfrac{\mu\sin\gamma}{Vr^2} - \dfrac{V\sin\gamma}{r} \\ \dfrac{L_\alpha + T_\alpha\sin\alpha + T\cos\alpha}{mV} \\ \dfrac{T_{\delta T}\sin\alpha}{mV} \\ \dfrac{L_h + T_h\sin\alpha}{mV} + \dfrac{2\mu\cos\gamma}{Vr^3}r_h - \dfrac{V\cos\gamma}{r^2}r_h \end{bmatrix} \tag{B8}$$

$$\Xi_2 = [\pi_{21} \quad \pi_{22} \quad \pi_{23} \quad \pi_{24} \quad \pi_{25}] \tag{B9}$$

where

$$\pi_{21} = \begin{bmatrix} \dfrac{L_{VV} + T_{VV}\sin\alpha}{mV} - \dfrac{2(L_V + T_V\sin\alpha)}{mV^2} + \dfrac{2(L + T\sin\alpha)}{mV^3} - \dfrac{2\mu\cos\gamma}{V^3r^2} \\ -\dfrac{\mu\sin\gamma}{V^2r^2} - \dfrac{\sin\gamma}{r} \\ \dfrac{L_{V\alpha} + T_{V\alpha}\sin\alpha + T_V\cos\alpha}{mV} - \dfrac{L_\alpha + T_\alpha\sin\alpha + T\cos\alpha}{mV^2} \\ \dfrac{T_{V\delta T}\sin\alpha}{mV} - \dfrac{T_{\delta T}\sin\alpha}{mV^2} \\ \dfrac{L_{Vh} + T_{Vh}\sin\alpha}{mV} - \dfrac{L_h + T_h\sin\alpha}{mV^2} - \dfrac{2\mu\cos\gamma}{V^2r^3}r_h - \dfrac{\cos\gamma}{r^2}r_h \end{bmatrix} \tag{B10}$$

$$\pi_{22} = \begin{bmatrix} -\mu\sin\gamma/(V^2r^2) - \sin\gamma/r \\ \mu\cos\gamma/(Vr^2) - V\cos\gamma/r \\ 0 \\ 0 \\ -(2\mu\sin\gamma/(Vr^3))r_h + (V\sin\gamma/r^2)r_h \end{bmatrix} \tag{B11}$$

$$\pi_{23} = \begin{bmatrix} \dfrac{L_{V\alpha} + T_{V\alpha}\sin\alpha + T_V\cos\alpha}{mV} - \dfrac{L_\alpha + T_\alpha\sin\alpha + T\cos\alpha}{mV^2} \\ 0 \\ \dfrac{L_{\alpha\alpha} + T_{\alpha\alpha}\sin\alpha + 2T_\alpha\cos\alpha - T\sin\alpha}{mV} \\ \dfrac{T_{\alpha\delta T}\sin\alpha + T_{\delta T}\cos\alpha}{mV} \\ \dfrac{L_{\alpha h} + T_{\alpha h}\sin\alpha + T_h\cos\alpha}{mV} \end{bmatrix} \tag{B12}$$

$$\pi_{24} = \begin{bmatrix} T_{V\delta T}\sin\alpha/(mV) - T_{\delta T}\sin\alpha/(mV^2) \\ 0 \\ (T_{\alpha\delta T}\sin\alpha + T_{\delta T}\cos\alpha)/(mV) \\ T_{\delta T\delta T}\sin\alpha/(mV) \\ T_{\delta Th}\sin\alpha/(mV) \end{bmatrix} \tag{B13}$$

$$\pi_{25} = \begin{bmatrix} \dfrac{L_{Vh} + T_{Vh}\sin\alpha}{mV} - \dfrac{L_h + T_h\sin\alpha}{mV^2} - \dfrac{2\mu\cos\gamma}{V^2r^3}r_h - \dfrac{\cos\gamma}{r^2}r_h \\ -\dfrac{2\mu\sin\gamma}{Vr^3}r_h + \dfrac{V\sin\gamma}{r^2}r_h \\ \dfrac{L_{\alpha h} + T_{\alpha h}\sin\alpha + T_h\cos\alpha}{mV} \\ \dfrac{T_{\delta Th}\sin\alpha}{mV} \\ \dfrac{L_{hh} + T_{hh}\sin\alpha}{mV} - \dfrac{6\mu\cos\gamma}{Vr^4}r_h^2 + \dfrac{2V\cos\gamma}{r^3}r_h^2 \end{bmatrix} \tag{B14}$$

Acknowledgment

This research has been supported by the Federal Aviation Administration and NASA under FAA Grant 95-G-0011.

References

[1]Ray, L. R., and Stengel, R. F., "Stochastic Robustness of Linear-Time-Invariant Control Systems," *IEEE Transactions of Automatic Control*, Vol. 36, No. 1, 1991, pp. 82–87.

[2]Ray, L. R., and Stengel, R. F., "A Monte Carlo Approach to the Analysis

of Control System Robustness," *Automatica*, Vol. 29, No. 1, 1993, pp. 229–236.

[3]Marrison, C. I., and Stengel, R. F., "Stochastic Robustness Synthesis Applied to a Benchmark Control Problem," *International Journal of Robust and Nonlinear Control*, Vol. 5, No. 1, 1995, pp. 13–31.

[4]Marrison, C. I., and Stengel, R. F., "Robust Control System Design Using Random Search and Genetic Algorithms," *IEEE Transactions on Automatic Control*, Vol. 42, No. 1, 1997, pp. 835–839.

[5]Stengel, R. F., and Wang, Q., "Searching for Robust Minimal-Order Compensators," *Proceedings of 1998 American Control Conference*, American Automatic Control Council, Piscataway, NJ, 1998, pp. 3138–3142.

[6]Wang, Q., and Stengel, R. F., "Robust Control of Nonlinear Systems with Parametric Uncertainty," *Proceedings of 1998 Conference on Decision and Control*, Inst. of Electrical and Electronics Engineers, Piscataway, NJ, 1998, pp. 3341–3346.

[7]Marrison, C. I., and Stengel, R. F., "Design of Robust Control Systems for a Hypersonic Aircraft," *Journal of Guidance, Control, and Dynamics*, Vol. 21, No. 1, 1998, pp. 58–63.

[8]Isidori, A., *Nonlinear Control Systems*, Springer–Verlag, Berlin, 1989, pp. 137–277.

[9]Singh, S. N., and Rugh, W. J., "Decoupling in a Class of Nonlinear Systems by State Variable Feedback," *Journal of Dynamic Systems, Measurement and Control*, Vol. 94, No. 4, 1972, pp. 323–329.

[10]Lane, S. H., and Stengel, R. F., "Flight Control Design Using Nonlinear Inverse Dynamics," *Automatica*, Vol. 24, No. 4, 1988, pp. 471–483.

[11]Kalos, M. H., and Whitlock, P. A., *Monte Carlo Methods*, Wiley, New York, 1986, pp. 92–115.

[12]Shaughnessy, J. D., Pinckney, S. Z., McMinn, J. D., Cruz, C. I., and Kelley, M.-L., "Hypersonic Vehicle Simulation Model: Winged-Cone Configuration," NASA TM 102610, Nov. 1990.

[13]Goldberg, D. E., *Genetic Algorithms in Search, Optimization, and Machine Learning*, Addison Wesley, Reading, MA, 1989, pp. 60–86.